PRAMANA
—journal of
physics

Vol. 49, No. 5,
November 1997
pp. 461–478

Polarization and dichroism in atomic Auger spectroscopy following absorption of circularly polarized light

S SEN
Department of Physics and Meteorology, Indian Institute of Technology, Kharagpur 721 302, India
Email: sandphy@phy.iitkgp.ernet.in

MS received 11 April 1997; revised 7 October 1997

Abstract. Spin resolved Auger current is shown to be different for the absorption of left and right circularly polarized light. This current is produced in non-radiative spontaneous decay of photoexcited atoms or of excited atomic photoions. Circular dichroism in such polarized Auger electrons exists even in the absence of spin–orbit interaction. Physical and geometrical conditions, necessary for the occurrence of dichroic effects in atomic Auger spectroscopy, have been obtained. Calculations for Ba and Xe show that the effect is substantially large and can be readily observed.

Keywords. Spin-polarization; circular dichroism; orientation and alignment parameters; spin orbit interaction (SOI); Auger electron.

PACS No. 33.55

1. Introduction

In a recent paper [1], we have investigated the existence of dichroic effects in Auger electron spectroscopy (AES), following absorption of circularly polarized (CP) light in a free and unpolarized rotating linear molecule in electric dipole ($E1$) approximation. The photoexcited molecule AB^* or the excited photoion AB^{+*} in eq. (I.1) of [1] remembers the helicity of the absorbed photon which created it. This memory is reflected in its subsequent radiationless decay. In other words, it means that the spin-resolved Auger current produced after the absorption of left circularly polarized (LCP) radiation is different from that emitted when the absorbed electromagnetic wave is right circularly polarized (RCP).

In the next section of this paper we show that the conditions in which one can observe circular dichroism (CD) in Auger spectroscopy of atoms are almost identical to those [1] of linear molecules. We, in particular, find that in order to study this effect in atoms, it is necessary to analyse spin of Auger electrons also but without taking the spin-orbit interaction (SOI) into account. Dichroism may exist both in the spin-resolved differential as well as integrated Auger currents. It does not necessarily vanish in any particular experimental configuration, including those which correspond to achiral geometries [2]. However, the dichroic effect will be absent if the integrated Auger current is spin-resolved perpendicular to the direction of incidence of CP ionizing radiation or Auger electrons are polarized perpendicular to the plane which contains both departing

electrons as well as incident photon beam. (These two and other experimental geometries are explained below in figure 1.) Another important feature is that the CD in Auger spectroscopy both of atoms and of rotating linear molecules is described by the same set of equations containing up to three parameters. But the dynamical factors to be used for the former are, of course, naturally different from those needed for the latter targets.

In order to see the magnitude of dichroic effects in atomic AES, we have performed in § 3 of this paper numerical calculations for Ba and Xe atoms. Here, the Auger currents are produced following photoionization in $5p$ and $4d$ subshells of Ba and Xe, respectively, after the absorption of a CP photon. In that section we have also analysed the spin polarization of Auger electrons emitted from these two atoms in the absence of SOI. The conclusion of this work is presented in § 4.

2. Theory for circular dichroism in atomic Auger spectroscopy

The processes of interest to us in the present paper are

$$h\nu_r + X(L_0S_0J_0M_0) \rightarrow X^*(LSJM) \tag{1a}$$

followed by

$$X^*(LSJM) \rightarrow X^+(L_fS_fJ_fM_f) + e_a(\mathbf{k}_a;\ \hat{u}_a\mu_a) \tag{1b}$$

and

$$h\nu_r + X(L_0S_0J_0M_0) \rightarrow X^{+*}(LSJM) + e_p \tag{2a}$$

followed by

$$X^{+*}(LSJM) \rightarrow X^{++}(L_fS_fJ_fM_f) + e_a(\mathbf{k}_a;\ \hat{u}_a\mu_a) \tag{2b}$$

caused by the absorption of a photon of frequency ν_r in a free and unpolarized atom X. While X^* in (1) is the photoexcited neutral atom, X^{+*} in (2) is the excited photoion formed after the emission of photoelectron e_p which remains unobserved. Emission of the Auger electron e_a results in the formation of residual singly and doubly charged atomic ions X^+ and X^{++} in (1b) and (2b), respectively. (L_0, L, L_f) and (S_0, S, S_f) are the respective total orbital and spin angular momenta of (X, X^*, X^+) in (1) and of (X, X^{+*}, X^{++}) in (2). We also have in these equations the total angular momenta $\mathbf{J}_0 = \mathbf{L}_0 + \mathbf{S}_0$, $\mathbf{J} = \mathbf{L} + \mathbf{S}$ and $\mathbf{J}_f = \mathbf{L}_f + \mathbf{S}_f$ with their respective projections $M_0\hbar$, $M\hbar$ and $M_f\hbar$ along the polar axis of the space-frame. Further in (1b) and (2b), $\mathbf{k}_a(k_a, \hat{k}_a)$ is the propagation vector of Auger electron moving with kinetic energy $\epsilon_a = \hbar^2k_a^2/2m$ and the component $\mu_a\hbar(\mu_a = \pm 1/2)$ of its spin angular momentum along the spin quantization direction $\hat{u}_a(\theta_a, \phi_a)$ defined in the photon-frame coordinate system OXYZ in figure 1(a).

Spin polarization in the presence of spin-dependent interactions of Auger electrons emitted in the non-radiative decay of an inner atomic shell vacancy created in the excitation or ionization of unpolarized atoms by particle impact or photon absorption has theoretically been considered by many workers [3–7]. The atomic expressions derived in [3–7] can readily be written in the form of eq. (II.20). The Auger decay matrix elements

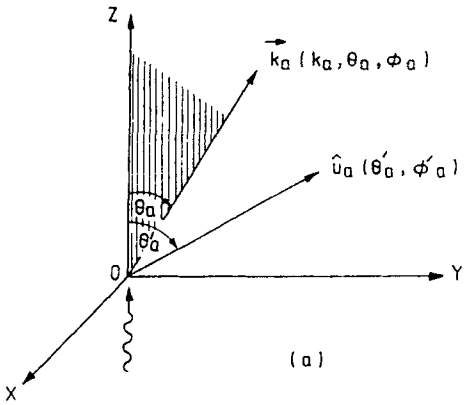

Figure 1(a). General geometry of an experiment used to study spin-polarization of Auger electrons. OXYZ is the photon (or laboratory) frame of reference. Its polar (OZ)-axis is along the direction of incidence of circularly polarized or unpolarized photon absorbed before Auger emissions. (If incident radiation is linearly polarized then its electric field vector is in the direction of OZ). Reaction (or scattering) plane contains the OZ-axis and the propagation vector $\mathbf{k}_a(k_a, \theta_a, \phi_a)$ of Auger electrons. Spin of Auger electrons is quantized along $\hat{u}_a(\theta'_a, \phi'_a)$. If the OX-axis lies in the scattering plane, then $\mathbf{k}_a(k_a, \theta_a, \phi_a = 0, \pi)$.

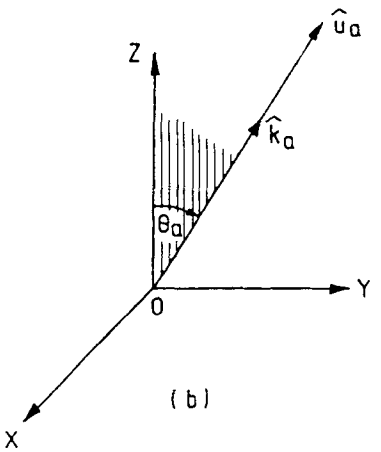

Figure 1(b). Experimental geometry for observing longitudinally polarized Auger electrons. Here $\hat{u}_a \| \hat{k}_a$ such that $\theta'_a = \theta_a$, $\phi'_a = \phi_a$.

A_{lj} to be used for atoms in eq. (II.20) are now given by

$$A_{lj}(J_f; J) = (-i)^l e^{i\sigma_l} \sqrt{(2l+1)(2j+1)} \langle J_f j | V_c | J \rangle \tag{3a}$$

with

$$A = \sum_{lj} |\langle J_f j | V_c | J \rangle|^2 \tag{3b}$$

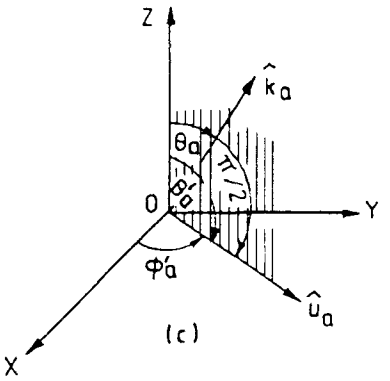

Figure 1(c). Configuration of an experiment for observing Auger electrons, with transverse polarization in the scattering plane. In this case $\theta'_a = \theta_a + \pi/2$ and $\phi' = \phi_a$ for $0 \leq \theta_a \leq \pi/2$; $\theta'_a = \theta_a - 3\pi/2$ and $\phi'_a = \phi_a + \pi$ for $\pi/2 \leq \theta_a \leq \pi$.

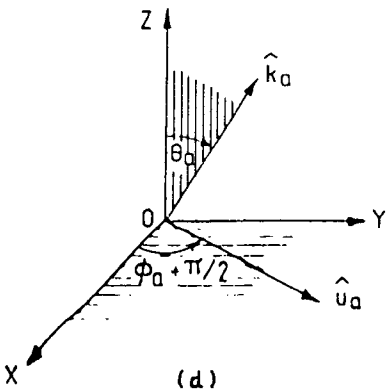

Figure 1(d). Experimental arrangement for observing Auger electrons with transverse polarization perpendicular to the scattering plane. In this geometry, $\theta'_a = \pi/2$, $\phi'_a = \phi_a + \pi/2$.

and

$$\sigma_a = K_a A\sqrt{2J+1}\langle T(J;m_r)^+_\infty\rangle \tag{3c}$$

is the spin-unresolved, integrated Auger current with constant K_a defined in eq. (II.2). In (3a) σ_l is the Coulomb phase [8] for the lth partial wave of Auger electron; both in (3b) and (3c), V_c is the inter-electronic Coulomb interaction. The state multipoles [9] $\langle T(J;m_r)^+_{KQ}\rangle$, present in the definition (II.13) of the normalized statistical tensor $\rho_{KQ}(J;m_r)$ needed for the angle- and spin-resolved Auger electron spectroscopy (ASRAES) expression (II.20), can be readily obtained from the expressions developed in the paper II by using the procedure explained in ref. [18]. The parameter m_r in (3c) specifies the state of polarization of the absorbed photon ($m_r = 0$ for plane and $m_r = \pm 1$ for circularly polarized light).

In order to obtain an expression for CD in atomic AES, we first need to eliminate the effects of SOI from the second step of each of the processes (1) and (2). That is, from

(X^*, X^+, plus Auger continuum) in (1b) and (X^{+*}, X^{++}, plus Auger continuum) in (2b). It is readily done by transforming the Auger decay matrix element (3a), occurring in the distribution (II.20), from the *j–j* to L–S coupling with the help of the relations (4.20) and (4.21) given in ref. [10]. This yields

$$\langle J_f j|V_c|J\rangle \equiv \langle (L_f S_f) J_f (l\,\tfrac{1}{2})\, j|V_c|(LS)J\rangle$$
$$= \sqrt{(2j+1)(2J_f+1)(2L+1)(2S+1)} \begin{Bmatrix} L_f & l & L \\ S_f & \frac{1}{2} & S \\ J_f & j & J \end{Bmatrix} \langle (L_f l)L|V_c|L\rangle. \tag{4}$$

Next we substitute (3a), (II.13), (3c), (4) and the geometrical factor (II.19) in eq. (II.20). The sum over j, j', J_f can then be analytically performed using an identity from ref. [11]. We then find, after some additional simplifications, that the angular distribution of spin-resolved Auger electrons emitted from atoms in the absence of SOI in the decay processes (1b) and (2b) is described by

$$\frac{d\sigma_a(m_r; \hat{u}_a \mu_a)}{d\hat{k}_a} = \frac{\sigma_a}{A} \sum_{\substack{ll' \\ KQ}} G(LSJ; L_f S_f; KQ; ll'; \hat{k}_a \hat{u}_a \mu_a) \rho_{KQ}(J; m_r) A_l(L_f, L)$$
$$A^*_{l'}(L_f, L). \tag{5}$$

Here the total Auger intensity σ_a is still obtained from (3c) with

$$A = \sum_l |\langle (L_f l)L|V_c|L\rangle|^2 \tag{6}$$

in place of that given by (3b). The Auger decay matrix element in L-S coupling is

$$A_l(L_f; L) = (-i)^l e^{i\sigma_l} \sqrt{2l+1}\, \langle (L_f l)L|V_c|L\rangle. \tag{7}$$

Further in (5),

$$G(LSJ; L_f S_f; KQ; ll'; \hat{k}_a \hat{u}_a \mu_a) = (-1)^{1+\mu_a+L+S+L_f+S_f+K+Q}$$
$$\times (2L+1)(2S+1)\sqrt{2K+1} \sum_{\substack{L_a M_{L_a} \\ S_a M_{S_a}}} \sqrt{(2L_a+1)(2S_a+1)} \begin{pmatrix} l & l' & L_a \\ 0 & 0 & 0 \end{pmatrix}$$
$$\times \begin{pmatrix} \frac{1}{2} & \frac{1}{2} & S_a \\ -\mu_a & \mu_a & 0 \end{pmatrix} \begin{pmatrix} L_a & S_a & K \\ M_{L_a} & M_{S_a} & -Q \end{pmatrix} \begin{Bmatrix} l & l' & L_a \\ L & L & L_f \end{Bmatrix} \begin{Bmatrix} \frac{1}{2} & \frac{1}{2} & S_a \\ S & S & S_f \end{Bmatrix}$$
$$\times \begin{Bmatrix} L & S & J \\ L & S & J \\ L_a & S_a & K \end{Bmatrix} Y^{M_{L_a}}_{L_a}(\hat{k}_a) Y^{M_{S_a}}_{S_a}(\hat{u}_a) \tag{8}$$

is the geometrical factor.

The form of the distribution (5) is identical to that given in eq. (I.4) of [1] for rotating linear molecules without including either SOI or the spin-rotation interaction (SRI).

Although, the dynamical terms are naturally different in the two cases, the geometrical factors differ merely in the replacement of the respective molecular quantum numbers N and N_f in ref. [1] by the atomic total orbital angular momenta L and L_f in the present case. This means that the analysis given in the paper I for angle and spin-resolved AES of rotating linear molecules in the absence of SOI and SRI becomes immediately applicable in a similar situation (i.e., in the absence of SOI) to atoms as well.

For example, the distribution (5) for atomic targets too is completely characterized in the form of eq. (I.7) by four independent parameters. These parameters are the spin-unresolved, total Auger intensity σ_a given by eqs (3c), (6), plus β_a, γ_a, δ_a obtained from the respective equations (I.8a–c) after making the changes already mentioned in the above paragraph.

The applicability of the ASRAES (I.7) in the present case means that even CD in Auger electron spectroscopy (AES) (i.e., CDAES) of atoms can be completely described by eqs (I.13)–(I.15). This, in other words, means that CD will exist in the AES of both atomic as well as of rotating linear molecular targets in identical, both kinematical as well as physical conditions and can be treated in these two entirely different targets on an equal footing. Its important properties are:

(a) It is present in free and achiral atomic targets.
(b) It is observable only in spin-resolved integrated and differential Auger currents.
(c) No spin-dependent interations in the bound and continuum electrons are involved in either of the Auger decay processes (1b) and (2b).
(d) It does not necessarily vanish even in achiral experimental geometries [2] containing either three vectors (k_a, $\hat{u}_a$, and the direction of incidence of the CP radiation) in a single plane in eq. (I.13) or only two vectors (photon and Auger electron spin quantization axis) in eq. (I.14).
(e) Properties (I.16a–d) of CD in AES are valid for atomic targets as well.
(f) We know from eq. (II.A13) that

$$\rho_{10}(J; -m_r) = -\rho_{10}(J; m_r)$$
$$\rho_{20}(J; -m_r) = \rho_{20}(J; m_r)$$

for orientation and alignment parameters respectively. Using these, we find from the distribution (I.7)

$$\frac{d\sigma_a(-m_r; \hat{u}_a, \pm\mu_a)}{d\hat{k}_a} = \frac{d\sigma_a(m_r; \hat{u}_a, \mp\mu_a)}{d\hat{k}_a}. \tag{9}$$

The spin-resolved, integrated Auger currents (I.9a), too has properties similar to (9).

(g) CD in AES (I.13) and (I.14) is such that

$$\frac{d\sigma_a^{CD}(\hat{u}_a, -\mu_a)}{d\hat{k}_a} = -\frac{d\sigma_a^{CD}(\hat{u}_a, \mu_a)}{d\hat{k}_a} \tag{10a}$$

and

$$\sigma_a^{CD}(\hat{u}_a, -\mu_a) = -\sigma_a^{CD}(\hat{u}_a, \mu_a) \tag{10b}$$

respectively.

3. Applications

3.1 *Spin-polarization and CD in the Auger decay of photoexcited atoms*

We have calculated in paper I, the spin-resolved, integrated Auger current, its degree of polarization, and the corresponding CD in AES in terms of the total Auger current emitted in the non-radiative decay of a photoexcited rotating linear molecule. These are given in table I in ref. [1] for 102 different transitions of the type (I.1a). The results of that table are directly applicable also to the Auger electrons emitted from an atomic target through the process (1) after replacing [as explained after eq. (8)] the molecular quantum number N by the atomic total orbital angular momentum quantum number L. That is, the successive values of N, S, J given in the respective 2nd, 3rd and 4th columns of table 1 in ref. [1] will now specify the quantum numbers L, S, J of the states of photoexcited atom X^* in eq. (1).

For example, the Auger emission process (1) corresponding to the state number 7 is

$$h\nu_r + X(J_0 = \tfrac{5}{2}) \rightarrow X^*(^2P_{3/2}) \rightarrow X^+(S_f = 0) + e_a,$$

to the state number 13 is

$$h\nu_r + X(J_0 = \tfrac{1}{2}) \rightarrow X^*(^2D_{3/2}) \rightarrow X^+(S_f = 0) + e_a,$$

and to the state number 31 is

$$h\nu_r + X(J_0 = 5) \rightarrow X^*(^3F_4) \rightarrow X^+(S_f = \tfrac{1}{2}) + e_a.$$

These processes have their values of J_0 specified by the columns 8th, 6th and 8th of table I [1], respectively. We further have from table I in ref. [1] that $\gamma_a \rho_{10}(J; m_r) = m_r/8$ for each of these transitions. Here [1], $m_r = 0$, $+1$, and -1 for LP, RCP and LCP radiation of frequency ν_r absorbed in the three processes, respectively. Substitution of this value of $\gamma_a \rho_{10}(J; m_r)$ in eq. (I.9a) gives the spin-resolved, integrated Auger current $\sigma_a(m_r; \hat{u}_a, \mu_a) = (1 - (1/4) m_r \mu_a \cos\theta'_a)\sigma_a/2$; in eq. (I.9b) gives the degree $p(m_r; \hat{u}_a) = -(1/4) m_r \cos\theta'_a$ of spin-polarization of this current; in eq. (I.14) gives its circular dichroism $\sigma_a^{CD}(\hat{u}_a, \mu_a) = (1/4)\sigma_a \mu_a \cos\theta'_a$. Here σ_a is the spin-unresolved, integrated Auger current defined by (3c), (6). These values of $\sigma_a(m_r; \hat{u}_a, \mu_a)$, $p(m_r; \hat{u}_a)$, and of $\sigma_a^{CD}(\hat{u}_a, \mu_a)$ are obtained when SOI is not taken into account in the second step of any of the three above-mentioned process.

3.2 *Spin-polarization and CD in AES of Ba*

Recently, Kuntze *et al* [12–14] have studied spin-polarization of photoelectrons

$$h\nu_r + \mathrm{Ba}(5p^6 6s^2\ ^1S_0) \rightarrow \mathrm{Ba}^{+*}(5p^5 6s^2\ ^2P_{1/2,3/2}) + e_p(k_p s_{1/2}, k_p d_{3/2,5/2}) \quad (11a)$$

and of Auger electrons

$$\mathrm{Ba}^{+*}(5p^5 6s^2\ ^2P_{1/2,3/2}) \rightarrow \mathrm{Ba}^{++}(5p^6 6s^2\ ^1S_0) + e_p(k_p, p_{1/2,3/2}) \quad (11b)$$

emitted sequentially in the interaction of a barium atom with CP radiation. This obviously corresponds to the general process (2) considered in this paper with $(L_0, S_0, J_0 = 0)$,

$(L = 1; S = 1/2; J = 1/2, 3/2)$ and $(L_f, S_f, J_f = 0)$ for Ba, Ba^{+*} and Ba^{++} respectively. In order to study spin polarization of these Auger electrons and their dichroic behaviour according to the prescription explained in this paper, we take SOI into account neither in the continuum nor in the bound electrons in the second step (11b) representing the Auger decay of Ba^{+*}. It is obvious from the expression (I.8b) that the parameter γ_a is always independent of Auger dynamics. However, if $L_f = 0$, as in the present case of Ba^{++}, then the parameters β_a and δ_a too cease to depend upon the Auger decay matrix elements (see, eqs (I.18)). Thus, for such states of the excited photoion Ba^{+*} in (11b), the last three of the four parameters $(\sigma_a, \beta_a, \gamma_a, \delta_a)$ needed to describe angle and spin-resolved AES of Ba atom by eq. (I.7) become independent of the dynamical factors. The values of these three parameters are then readily calculated from eqs (I.8) (after replacing the respective molecular quantum numbers N and N_f by atomic orbital angular momenta L and L_f) to be

$$\beta_a = 0, \quad \gamma_a = 1/3\sqrt{2}, \quad \delta_a = 2\sqrt{2}/3 \tag{12a}$$

for $J = 1/2$ and

$$\beta_a = -\frac{1}{2}, \quad \gamma_a = -\frac{\sqrt{5}}{6} \quad \delta_a = -\frac{1}{3\sqrt{5}} \tag{12b}$$

for $J = 3/2$.

It is well known (see, for example, eqs (I.A8) and (II.A13)) that a state with $J = 1/2$ of a photoexcited atom or molecule, or of excited photoion of these species, will only be oriented not aligned. Kuntze *et al* [12] have given normalized orientation and alignment parameters for $Ba^{+*}(5p^5 6s^2\ ^2P_{1/2,3/2})$. The values of these parameters appropriate for present application are obtained after multiplying those given by Kuntze *et al* [12] by $\sqrt{2J+1}$. This yields

$$\rho_{10}(J = \tfrac{1}{2};\ m_r = +1) = -0.38; \quad \rho_{20}(J = \tfrac{1}{2};\ m_r = \pm 1) = 0 \tag{13a}$$

for $J = 1/2$ and

$$\rho_{10}(J = \tfrac{3}{2};\ m_r = +1) = 0.46; \quad \rho_{20}(J = \tfrac{3}{2};\ m_r = \pm 1) = 0.14 \tag{13b}$$

for $J = 3/2$. These correspond, respectively, to the photons of energies 25.8 eV and 23.5 eV incident in the process (11a) [12].

Following [12–14], let us take the reaction plane, defined in figure 1 to contain the polar axis and the propagation direction $\hat{k}_a(\theta_a, \phi_a)$ of the Auger electron, to be the X-Z plane of our photon-frame of reference. Then, obviously, the Auger electron moves out in direction $\hat{k}_a(\theta_a, \phi_a = 0)$. The three components

$$p_x = \frac{3}{4} \frac{\delta_a \rho_{10}(J; m_r) \sin 2\theta_a}{1 + \beta_a \rho_{20}(J; m_r) P_2(\cos\theta_a)}, \tag{14a}$$

$$p_y = 0, \tag{14b}$$

$$p_z = -\frac{\gamma_a - \delta_a P_2(\cos\theta_a)}{1 + \beta_a \rho_{20}(J; m_r) P_2(\cos\theta_a)} \rho_{10}(J; m_r) \tag{14c}$$

of the Auger electron polarization **p** specific to this frame of reference are readily obtained from eqs (I.10) and (I.11). Equation (14) immediately means that, if SOI is not

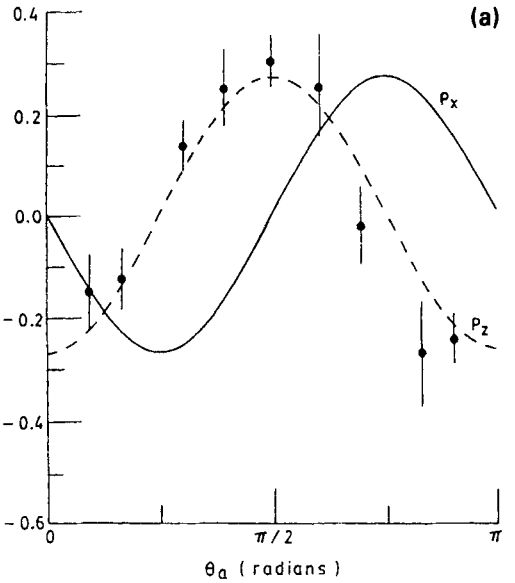

Figure 2(a). Variation of p_x and p_z components of the polarization vector of Auger electrons with the angle θ_a between directions of their propagation and of incidence of CP ionization radiation. These electrons are ejected in the non-radiative decay (11b) of excited photoion $Ba^{+*}(5p^5\,^2P_{1/2})$. Values shown have been calculated by substituting eqs (12a), (13a) in (14a, c). Circles (with error bars) are the values of p_z measured by Kuntze *et al* [12–14].

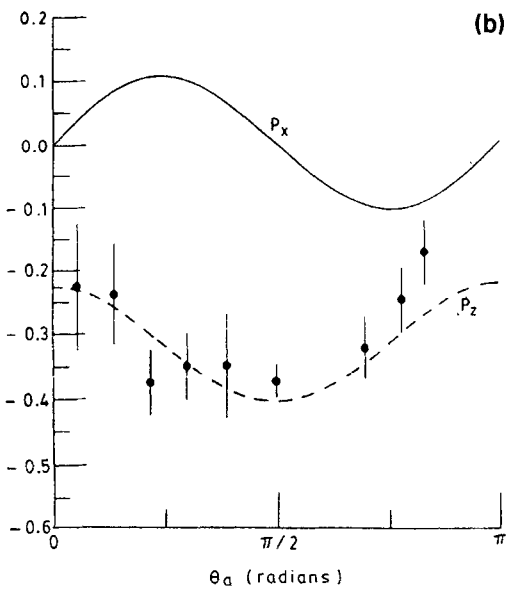

Figure 2(b). Same as figure 2(a), but for electrons ejected in the non-radiative decay (11b) of excited photoion $Ba^{+*}(5p^5\,^2P_{3/2})$. These values have been calculated by substituting eqs (12b), (13b) in (14a, c).

included in (11b), the Auger electrons do not have any polarization perpendicular to the scattering plane (see figure 1(d)). The last result, which was initially derived by Klar [3] in the context of atoms, is applicable to all states of photoexcited atom X^* and molecule AB^* in (1) and (I.1a) respectively, as well as of the excited atomic photoion X^{+*} in (2) and molecular photoion AB^{+*} in (I.1b,c).

Figure 2(a) contains X- and Z-components of the polarization vector **p** of Auger electrons emitted making an angle θ_a with the CP photon beam incident in the process (11b) with $J = 1/2$. These have been obtained by substituting (12a) and (13a) in (14). As both β_a and ρ_{20} vanish for $J = 1/2$, the denominator in eq. (14) is, therefore, equal to one for this case. We find from figure 2(a) that, whereas the maximum magnitude of each of the two components p_x and p_z is about 0.27, these are respectively antisymmetric and symmetric about $\theta_a = \pi/2$.

The values of the components p_x and p_z of the polarization vector **p** obtained by substituting (12b) and (13b) in (14) are shown in figure 2(b). These obviously correspond to $J = 3/2$ in the Auger transition (11b). Here too we find that, similar to figure 2(a), p_x and p_z are respectively antisymmetric and symmetric with respect to $\theta_a = \pi/2$. Moreover, $|p_x(J = 1/2)|_{max} > |p_x(J = 3/2)|_{max}$, but $|p_z(J = 1/2)|_{max} < |p_z(J = 3/2)|_{max}$. The most significant effects on polarization of Auger electrons of an increase in the total angular momentum of Ba^{+*}, which results both in orientation as well as in alignment of $p_{3/2}$ vacancy, are that (i) the maximum magnitude of $p_x(J = 3/2)$ is much smaller than that of $p_x(J = 1/2)$, $p_z(J = 1/2)$, and of $p_z(J = 3/2)$; (ii) $p_z(J = 3/2) < 0$ for all directions of propagation of Auger electrons in the X-Z plane (i.e., for all values of θ_a).

In order to see the effect of SOI in the second step of the process (11), we have calculated the parameters β_a, γ_a, δ_a, and ξ_a also from eqs (II.22). As $J_f = 0$ and a single p-partial wave of Auger electron contributes in the process (11b), all of the four parameters in eqs (II.22) become independent of Auger dynamics.

We find in this case that, while $\xi_a = 0$, each of the β_a, γ_a, and δ_a have values equal to those given by (12a) and (12b) for $J = 1/2$ and $3/2$, respectively. Consequently, with normalized orientation and alignment parameters taken from (13a) for $J = 1/2$ and from (13b) for $J = 3/2$ states of Ba^{+*}, the Cartesian components of the polarization vector of Auger electron obtained from eq. (II.27) also become identical to those given in (14) in this paper and shown in figure 2(a) and 2(b) herein.

Kuntze *et al* have measured p_y [13, 14] and p_z [12–14] both for $J = 1/2$ and $3/2$ in the process (11). These measurements [12–14] of p_z have been shown by open circles (along with error bars) in figure 2 in the present paper. On comparing the measured values [12–14] of p_z with those calculated in the present paper (and shown by the continuous curve in figure 2), we find that there is good agreement between the two, both in shape as well as magnitude. The same is true for p_y which has been measured [13, 14] to be zero. This agreement between theory and experiment shows that if the dynamics does not contribute to a particular Auger decay process, then the theoretical results obtained without SOI agree with those calculated and measured taking SOI into account.

Figures 3(a) and 3(b) contain the $\sigma_a^{CD}(\hat{u}_a, \mu_a)/\sigma_a$ in the spin-resolved, integrated Auger current produced in the respective decay of $J = 1/2$ and $J = 3/2$ states of Ba^{+*} in the process (11b). These have, respectively, been calculated by substituting (12) and (13) in (I.14). In each of the figures 3, curve 1 corresponds to the projection $-(1/2)\hbar$ and curve 2 to $+(1/2)\hbar$ of the spin-angular momentum of the Auger electron along the quantization

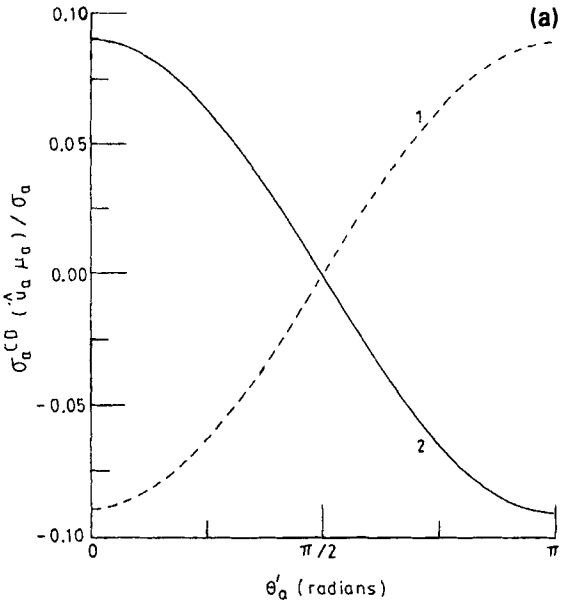

Figure 3(a). Variation of the ratios of CD in spin-resolved, integrated Auger current to the total (spin-unresovled) Auger intensity with the polar angle θ'_a between the spin-quantization direction of Auger electrons and the CP photon beam. These electrons are ejected in the non-radiative decay (11b) of the excited photoion $Ba^{+*}(5p^5\,{}^2P_{1/2})$. Ratios in this figure are calculated by substituting eqs (12a), (13a) in (I.14). Curve 1: $\mu_a = -1/2$; Curve 2: $\mu_a = +1/2$.

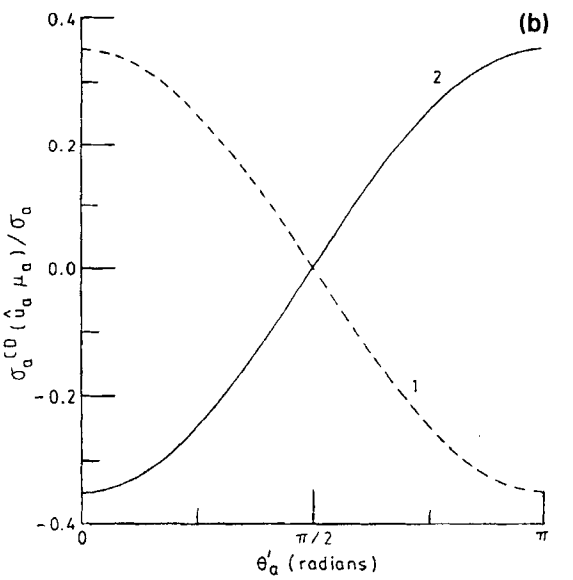

Figure 3(b). Same as figure 3(a), but for electrons emitted in the non-radiative decay (11b) of the excited photoion $Ba^{+*}(5p^5\,{}^2P_{3/2})$. Ratios in this figure are calculated by substituting eqs (12b), (13b) in (I.14).

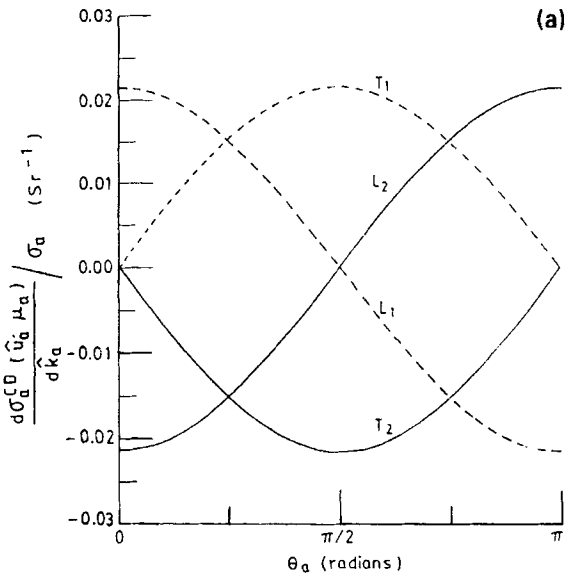

Figure 4(a). Variation of the ratios of CD in spin-resolved, differential Auger current to the total (spin-unresolved) Auger intensity with the angle θ_a between the outgoing electron and the CP radiation. These electrons are emitted in the non-radiative decay (11b) of $Ba^{+*}(5p^5\,^2P_{1/2})$. Curves $L_1(\mu_a = -1/2)$ and $L_2(\mu_a = +1/2)$ are calculated by substituting eqs (12a), (13a) in (I.16a) for longitudinal polarization of Auger electrons. Curves $T_1(\mu_a = -1/2)$ and $T_2(\mu_a = +1/2)$ are obtained by substituting eqs (12a), (13a) in (I.16b) for transverse polarization of Auger electrons in the reaction plane. (Here $\mu_a = \pm 1/2$ is the projection of Auger electrons spin along the quantization direction $\hat{u}_a$.)

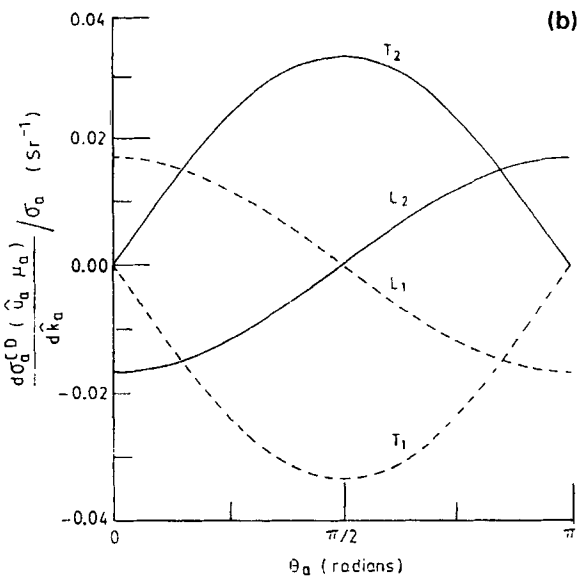

Figure 4(b). Same as figure 4(a) but for Auger electrons emitted in the non-radiative decay (11b) of the excited photoion $Ba^{+*}(5p^5\,^2P_{3/2})$. These ratios are calculated by substituting (12b), (13b) in (I.16a) for L_1 and L_2 and in (I.16b) for T_1, T_2.

direction which makes angle θ'_a with the incident CP light (see, figure 1(a)). The curves in each figure obviously obey the property (10b). Although, the magnitude of $\sigma_a^{CD}(\hat{u}_a, \mu_a)/\sigma_a$ in each of the figures 3 is within the experimentally measurable limit, the CD for $J = 3/2$ (in figure 3(b)) is almost four times that when $J = 1/2$ (in figure 3(a)) state of Ba^{+*}.

The ratio of the CD in spin-resolved differential Auger current (i.e., $d\sigma_a^{CD}(\hat{u}_a, \mu_a)/d\hat{k}_a$) to that of the total Auger intensity (σ_a) for different experimental geometries is shown in figure 4. Figure 4(a) corresponds to the decay of $Ba^{+*}(^2P_{1/2})$ state and is obtained by substituting (12a), (13a) in (I.16); whereas, figure 4(b) is for the Auger electrons emitted from $Ba^{+*}(^2P_{3/2})$ calculated by combining (12b), (13b) and (I.16). Curves $L_1(\mu_a = -1/2)$ and $L_2(\mu_a = +1/2)$ in both of these figures are for longitudinally polarized Auger electrons corresponding to eq. (I.16a). Similarly, the remaining two curves $T_1(\mu_a = -1/2)$ and $T_2(\mu_a = +1/2)$ in each of the figures 4(a) and 4(b) give us CD in spin-resolved differential Auger current for transverse experimental arrangement of eq. (I.16b). That is, L_1 and L_2 are for $\hat{u}_a \| \hat{k}_a$; whereas, T_1 and T_2 are for $\hat{u}_a \perp \hat{k}_a$. These two cases correspond to the experimental geometries shown in figures 1(b) and 1(c), respectively, wherein the Auger electron spin quantization direction $\hat{u}_a$ and its propagation vector $\hat{k}_a$ are in the plane which also contains the CP incident photon beam. Furthermore, all the curves in the figures 4(a) and 4(b) satisfy the property (10a). This means that, for all values of the angle θ_a between the direction of ejection of Auger electron and of incidence of CP radiation, L_1 and T_1 are always negative of L_2 and T_2 respectively. Finally, the ratios of the CD in spin-resolved differential Auger current to total Auger intensity in the figures 4(a) and 4(b) are well within the measurable limits of present experimental facilities.

3.3 *Spin-polarization and CD in AES of Xe*

The following photoionization process

$$h\nu_r + \mathrm{Xe}(4d^{10}5s^25p^6\,{}^1S_0) \rightarrow \mathrm{Xe}^{+*}(4d^95s^25p^6\,{}^2D_{5/2}) + e_p(k_p p_{1/2}, k_p f_{5/2,7/2}) \tag{15a}$$

in Xe succeeded by the spontaneous, non-radiative decay

$$\mathrm{Xe}^{+*}(4d^95s^2\,5p^6\,{}^2D_{5/2}) \rightarrow \mathrm{Xe}^{++}(4d^{10}5s^05p^6\,{}^1S_0) + e_p(k_a d_{5/2}) \tag{15b}$$

of the excited photoion Xe^{+*} has been studied by several workers, both theoretically as well as experimentally. More recently, Kammerling and Schmidt [15] have measured one-photon two-step, double ionization for (15) and theoretically studied [15, 16] both angular and spin-correlation between photo- and Auger-electrons emitted sequentially in the above process.

The values of the three polarization parameters obtained from eqs (I.8) for this case is

$$\beta_a = -\frac{2}{\sqrt{21}}, \quad \gamma_a = -\frac{1}{3}\sqrt{\frac{7}{10}}, \quad \delta_a = -\frac{2}{3}\sqrt{\frac{2}{35}}. \tag{16a}$$

These parameters are independent of the Auger decay dynamics because we have, in the present case $L_f = 0$ and the Auger electron is represented by a single $d(l = 2)$-partial

wave in eq. (15b). Since $J_f = 0$ as well, eqs (II.22) which includes SOI in the Auger decay process (15b) will also yield the values of β_a, γ_a, δ_a given in (16a), with $\xi_a = 0$ (obtained from eq. (II.22d)). Thus similar to the case of Ba, discussed earlier, the SOI does not contribute to the second step in double ionization (15) of Xe.

In order to calculate the components of the polarization vector of Auger electrons and CD for (15b), we need to know both orientation and alignment parameters $\rho_{10}(J; m_r)$ and $\rho_{20}(J; m_r)$, respectively. These have been calculated herein using the photoionization matrix elements given by Kammerling and Schmidt [15]. The expression used in ref. [15] for the integrated cross-section for photoionization (15a) is [16]

$$\sigma(4d_{5/2}) = \frac{8\pi^4}{\omega c}\,(|d'(p_{3/2})|^2 + |d'(f_{5/2})|^2 + |d'(f_{7/2})|^2).$$

Here ω is the energy of the photon incident in (15a) and c (= 137) is the speed of light in atomic unit (a.u.); d' are the photoionization amplitudes in electric dipole ($E1$) approximation. But the theoretical frame-work developed in ref. [1] and [17] gives the integrated photoionization cross-section for (15a) to be

$$\sigma(4d_{5/2}) = K_p(|d(p_{3/2})|^2 + |d(f_{5/2})|^2 + |d(f_{7/2})|^2),$$

with $K_p = 3\pi(e^2/\alpha_0 E_r^2)$ in absolute units. Here e is the electronic charge, α_0 the dimensionless fine structure constant and E_r the photon energy. Converting it to atomic units, we get $K_p = 3\pi c^2/\omega^2$. Therefore, in order to be able to use the $E1$ amplitudes given by Kammerling and Schmidt [15], we should first multiply them by $8\pi^3\omega/(3c^3)$. This 're-normalization' procedure will, however, only change the magnitude of $E1$ photoionization matrix elements, but their [15] phases will remain unaltered. Therefore, the magnitude of the $E1$ transition amplitudes we have used in calculating the orientation and alignment parameters for photoionization step (15a) are

$$d(p_{3/2}) = 1.459 \times 10^{-3}\ \text{a.u.},$$
$$d(f_{5/2}) = -1.385 \times 10^{-3}\ \text{a.u.},$$
$$d(f_{7/2}) = -5.010 \times 10^{-3}\ \text{a.u.},$$

with associated phases given in [15]. The corresponding normalized orientation and alignment factors for $Xe^{+*}(4p^9\,{}^2D_{5/2})$ are then readily obtained from (II.13) to be [18]:

$$\rho_{10}(J;\ m_r) = -1.86 m_r; \quad \rho_{20}(J;\ m_r) = 0.279(3m_r^2 - 2). \tag{16b}$$

Here [1], [17], $m_r = 0$ for LP and $m_r = \pm 1$ for CP light incident in (15a). The energy of the LP photon in experiment of [15] was 94.5 eV.

The X- and Z-components of the polarization vector **p** of Auger electrons emitted from Xe in the process (15) are shown in figure 5. The results have been computed by substituting (16) in (14). On comparing figures 2(b) and 5 we find that the nature of variation of p_x and p_z with the angle of emission θ_a of Auger electrons in the two figures is almost the same. It is because both orientation and alignment contribute to the polarization of Auger electrons in the non-radiative decay of $Ba^{+*}(^2P_{3/2})$ in (11b) and of $Xe^{+*}(^2D_{5/2})$ in (15b). However, the magnitude of p_z for Xe-Auger electron is much larger than for those coming out from Ba^{+*}, but p_x has almost equal magnitude in

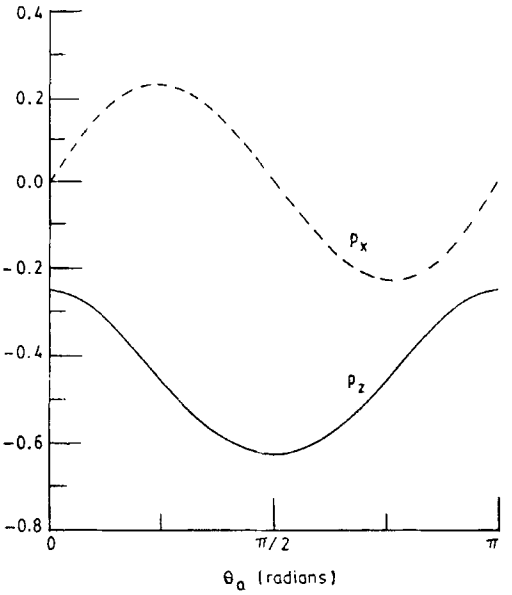

Figure 5. Same as figure 2(a) but for Auger electrons emitted in the non-radiative decay (15b) of excited photoion $Xe^{+*}(4p^9\,{}^2D_{5/2})$. These values have been calculated by substituting eq. (16) in (14a, c).

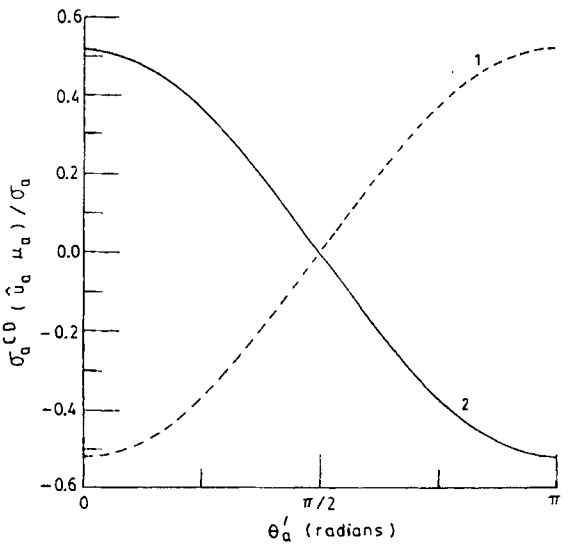

Figure 6. Same as figure 3(a) but for Auger electrons emitted in the non-radiative decay (15b) of excited photoion $Xe^{+*}(4p^9\,{}^2D_{5/2})$. These ratios are calculated by substituting eqs (16) in (I.14).

figures 2(a) and 5, which is almost twice of that given in figure 2(b) for $Ba^{+*}({}^2P_{3/2})$. This simply means that the degree of spin-polarization of Auger electrons emitted in (15) is expected to be much larger than those coming out from (11).

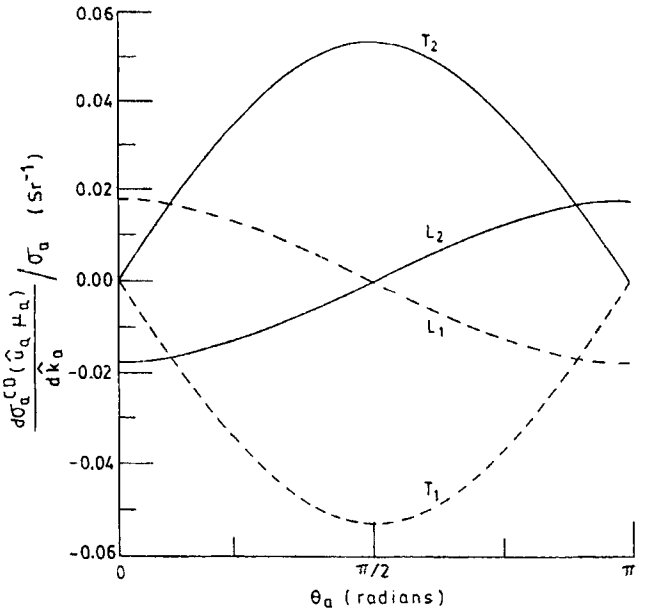

Figure 7. Same as figure 4(a) but for Auger electrons emitted in the non-radiative decay (15b) of excited photoion $Xe^{+*}(4p^9\,{}^2D_{5/2})$. These ratios are calculated by substituting eqs (16) in (I.16a) for L_1 and L_2 and in (I.16b) for T_1, T_2.

As far as we know, unfortunately, no experimental measurements or any other calculations for spin-polarization of Auger electrons emitted in the process (15) in Xe are available. Talkki *et al* [19] have computed those parameters which are needed in eq. (II.27b) to calculate p_y component of the polarization vector perpendicular to the reaction plane in the presence of SOI. But, for the transition (II.27b) in Xe^{+*}, p_y has already been shown to vanish identically elsewhere in this paper. Consequently, the results presented in figure 5 are the first theoretical prediction of the components p_x and p_z of the polarization vector **p** of Auger electrons emitted in the process (15) in Xe.

In the respective figures 6 and 7, we have shown the ratios of the CD in spin-resolved integrated and differential Auger currents to the total Auger intensity for the process (15). These have been calculated by substituting eq. (16) in (I.14) and (I.16), respectively. In figure 7, both longitudinal (L_1, L_2) as well as transverse (T_1, T_2) geometries, corresponding to eqs (I.16a) and (I.16b) respectively, have been considered. (These experimental arrangements are shown in the respective figures 1(b) and 1(c).) The magnitude of the ratios in these figures are usually larger than those of Ba shown in figures 3 and 4. Another interesting comparison between CD in Ba and Xe AES is that variations in figure 6 with respect to θ'_a and in figure 7 with respect to θ_a for $Xe^{+*}({}^2D_{5/2})$ are similar to those found for $Ba^{+*}({}^2P_{3/2})$ in figures 3(b) and 4(b), respectively.

4. Conclusion

In this paper, we have shown that the same set of equations describe angle- and spin-resolved AES following photoabsorption in both atoms as well as in rotating linear

molecules with or without including SOI in the second step of Auger emission. Although, the dynamical terms needed for atomic systems are naturally different from those for molecules, the geometrical factor, is however, identical in the two cases. We have, urther, shown that CD exists in the AES of both of these targets in almost identical physical as well as geometrical conditions and is, again, represented by the same equations which do not include SOI in the Auger decay dynamics. We have used these equations for calculating components of the polarization vector and CD for Auger electrons emitted from the excited photoions $Ba^{+*}(5p^5\,^2P_{1/2,3/2})$ and $Xe^{+*}(4p^9\,^2D_{5/2})$.

Our investigations show that if the total orbital angular momentum L_f as well as the total angular momentum J_f of the doubly charged ion left after Auger emission is zero (i.e., it is in its $^1S_0$ state) and the departing electron is represented by a single partial wave, then the degree of spin polarization of Auger electrons is not affected by the absence or presence of SOI in bound and/or continuum electrons. The Auger electrons in this case are spin-resolved if and only if their emission is preceeded by the absorption of CP light, whether or not SOI is included. In such experiments, polarization of Auger electrons is confined only to the plane which contains both the outgoing electrons as well as the CP ionizing radiation, and vanishes identically in a direction perpendicular to this plane. In the three examples considered in this paper, the maximum magnitude of the p_z component of polarization vector along the photon beam is either equal to or larger than its p_x component perpendicular to the photon beam. Moreover, the degree of spin polarization of Auger electrons produced in the decay of $Xe^{+*}(4p^9\,^2D_{5/2})$ is much larger than of those emitted from either of the two states $(5p^5\,^2P_{1/2,3/2})$ of Ba^{+*}. The CD investigations performed here are useful for studying spin-resolved Auger spectroscopy, and for investigating the influence of SOI on Auger electrons. The circular dichroism calculated in this paper in the AES of Ba and Xe suggests that it is sufficiently larger and can be studied experimentally. In addition, being the difference of two aspects of almost equal values, CD studies provide more stringent test for theoretical models.

Acknowledgements

The author is thankful to the Council of Scientific and Industrial Research for the award of a Research Associateship.

References

[1] N Chandra and S Sen, *Phys. Rev.* **A48**, 2084 (1993) [This paper will henceforth be referred to as I and an equation number of this paper cited herein is enclosed in the parentheses with the letter I]
[2] G Schonhense, *Phys. Scr.* **T31**, 255 (1990)
[3] H Klar, *J. Phys.* **B13**, 4741 (1980)
[4] N M Kabachnik, *J. Phys.* **B14**, L377 (1981)
[5] K N Huang, *Phys. Rev.* **A26**, 2274 (1982)
[6] K Blum, B Lohmann and E Taute, *J. Phys.* **B19**, 3815 (1986)
[7] N M Kabachnik and O V Lee, *J. Phys.* **B22**, 2705 (1989)
[8] N Chandra, *Chem. Phys.* **108**, 301 (1986)
[9] K Blum, *Density matrix theory and applications* (Plenum, New York, 1981)
[10] R N Zare, *Angular momentum* (John Wiley, New York, 1988)

[11] D A Varshalovich, A N Moskalev and V K Khersonskii, *Quantum theory of angular momentum* (World Scientific, Singapore, 1988) [eq. (44) on page 474]
[12] R Kuntze, M Salzmann, N Bowering and U Heinzmann, *Phys. Rev. Lett.* **70**, 3716 (1993)
[13] R Kuntze, M Salzmann, N Bowering and U Heinzmann, *Z. Phys.* **D30**, 235 (1994)
[14] R Kuntze, M Salzmann, N Bowering, U Heinzmann, V K Ivanov and N M Kabachnik, *Phys. Rev.* **A50**, 489 (1994)
[15] B Kammerling and V Schmidt, *Phys. Rev. Lett.* **67**, 1848 (1991)
[16] B Kammerling and V Schmidt, *J. Phys.* **B26**, 1141 (1993)
[17] N Chandra and S Sen, *J. Chem. Phys.* **98**, 5242 (1993) [This paper will hence forth be referred to as II. An equation number of this paper cited herein is enclosed in the parentheses with letters II]
[18] In ref. [17], we have derived respective expression [(A11), (A11′)] and [(A13), (A13′)] for state multiples and normalized statistical tensors for photoion of a linear molecule rotating according to the Hund's coupling scheme (a) or (b). These expressions are applicable to the present atomic studies as well provided the following $\langle J;\ jl|F(j_t)|J_0;\ 1\rangle = (2J_0+1)^{-1/2}\sum_{J_T}(2J_T+1)\begin{Bmatrix} j & J & J_T \\ 1 & J_0 & j_t \end{Bmatrix}\langle J;\ jl|F(J_T)|J_0;\ 1\rangle$ definition, in place of that given in eq. (II.A10), of 'reduced' amplitude is used in eqs (II.A9)–(II.A13′). Here, the $E1$ ionization amplitude is taken from eq. (9) in N Chandra, *Phys. Rev.* **A42**, 4050 (1990)
[19] J Tulkki, N M Kabachnik and H Aksela, *Phys. Rev.* **A48**, 1277 (1993)